Research article

LUMINESCENCE
The Journal of Biological and Chemical Luminescence

Received: 20 August 2015, Revised: 25 March 2016, Accepted: 26 March 2016 Published online in Wiley Online Library: 5 May 2016

(wileyonlinelibrary.com) DOI 10.1002/bio.3148

Eu^{2+}-induced enhancement of defect luminescence of ZnS

Zhang Xiao-Bo[a,b]* and Wei Fu-Xiang[c]

ABSTRACT: The Eu^{2+}-induced enhancement of defect luminescence of ZnS was studied in this work. While photoluminescence (PL) spectra exhibited 460 nm and 520 nm emissions in both ZnS and ZnS:Eu nanophosphors, different excitation characteristics were shown in their photoluminescence excitation (PLE) spectra. In ZnS nanophosphors, there was no excitation signal in the PLE spectra at the excitation wavelength $\lambda_{ex} > 337$ nm (the bandgap energy 3.68 eV of ZnS); while in ZnS:Eu nanophosphors, two excitation bands appeared that were centered at 365 nm and 410 nm. Compared with ZnS nanophosphors, the 520 nm emission in the PL spectra was relatively enhanced in ZnS:Eu nanophosphors and, furthermore, in ZnS:Eu nanophosphors the 460 nm and 520 nm emissions increased more than 10 times in intensity. The reasons for these differences were analyzed. It is believed that the absorption of Eu^{2+} intra-ion transition and subsequent energy transfer to sulfur vacancy, led to the relative enhancement of the 520 nm emission in ZnS:Eu nanophosphors. In addition, more importantly, Eu^{2+} acceptor-bound excitons are formed in ZnS:Eu nanophosphors and their excited levels serve as the intermediate state of electronic relaxation, which decreases non-radiative electronic relaxation and thus increases the intensity of the 460 nm and 520 nm emission dramatically. In summary, the results in this work indicate a new mechanism for the enhancement of defect luminescence of ZnS in Eu^{2+}-doped ZnS nanophosphors.

Keywords: ZnS nanophosphor; defect luminescence; Eu^{2+} acceptor-bound exciton; electronic relaxation; the intermediate state

Introduction

ZnS is an excellent luminescence host material and, frequently, transition and rare-earth (RE) metal impurities are doped in the ZnS host to obtain impure luminescence. In recent years, however, it has been reported that doping of transition and RE metal impurities can greatly enhance the luminescence intensity of ZnS materials (1–5). For example, Yang *et al.* reported that emission intensities increased by about five to six times in ZnS nanocrystallites after doping with Ce, Y, Nd, Er and Tb metal ions (1). Sridevi *et al.* reported that the fluorescence intensities of ZnS nanoparticles, doped with La, Mn, Co. and Ni metal ions, were five to six times that of pure ZnS (2). Importantly, it has been reported more recently that doping of Eu^{2+} can increase the luminescence of ZnS materials (3–5). Ashwini *et al.* reported that the luminescence intensity in ZnS:Eu^{2+} nanoparticles was enhanced with increasing doping concentrations of Eu^{2+}. The reason for this increase is ascribed to an increase in defect sites and traps with the increasing number of Eu^{2+} ions doped into ZnS nanoparticles (3,4). Ma *et al.* reported that doping with Eu^{2+} promoted the emission intensity of bulk ZnS phosphors by 7–30 times, explained as the formation of Eu^{2+}-related defects (5). In short, luminescence enhancement in the Eu^{2+}-doped ZnS materials is ascribed to the introduction of defects and traps (3–5).

In this work, ZnS nanophosphors and Eu^{2+}-doped ZnS (ZnS:Eu) nanophosphors were prepared. The results from photoluminescence (PL) spectra showed that luminescence intensity was increased by more than 10 times in ZnS:Eu nanophosphors compared with that in ZnS nanophosphors. Reasons for this increase are analyzed here. We propose that in ZnS:Eu nanophosphors, electronic relaxation is via the excited levels of Eu^{2+} acceptor-bound excitons, which decreased non-radiative electronic relaxation from the conduction band (CB) to valence band (VB), thus increasing the luminescence intensity dramatically. This conclusion is quite different from previous explanations by other groups: that the introduction of defects and traps leads to luminescence enhancement in Eu^{2+}-doped ZnS materials (3–5).

Experimental

ZnS and ZnS:Eu nanophosphors were obtained by annealing the corresponding nanoparticle precursors, which had been prepared previously by chemical co-precipitation methods. The detailed preparation processes are similar to those described in (6). The precipitation of ZnS nanoparticles was performed starting from homogeneous solutions of zinc acetate ($Zn(CH_3COO)_2{\cdot}2H_2O$) at 0.3 M and thioacetamide (TAA) at 0.4 M. The two solutions were prepared in ultrapure water (18 MΩ) and heated separately to 80 °C. During heating, the TAA solution was kept at pH 2 by adding hydrochloric acid, so that TAA decomposition, which generated the sulfide anions, was controlled. The zinc salt solution and the TAA solution were mixed in a batch reactor with no agitation. The molecular ratio of Zn:S was 1:1.3. The reaction temperature and time were fixed at 80 °C and 30 min, respectively, and the mixed solution was still kept at pH 2 by adding hydrochloric acid.

* Correspondence to: Zhang Xiao-Bo, Department of Materials, Huaibei Normal University, Huaibei 235000, China. E-mail: zhangxiaobo@chnu.edu.cn

[a] Department of Materials, Huaibei Normal University, Huaibei 235000, China

[b] Key Laboratory of Excited State Physics, Changchun Institute of Physics, Chinese Academy of Sciences, Changchun 130022, China

[c] School of Materials Science and Engineering, China University of Mining and Technology, Xuzhou 221116, China

Abbreviations: CB, conduction band; IS, interstitial; PLE, photoluminescence excitation; SA, self-activated; VB, valence band; XRD, X-ray powder diffraction

LUMINESCENCE
The Journal of Biological and Chemical Luminescence

After that, the hydrolytic reaction of TAA was terminated by rapidly cooling the solution to <10 °C in an ice bath. Then, the cooled solution was centrifuged at 4000 rpm, washed three times with ultrapure water to eliminate TAA, and washed three times with isopropyl alcohol. The cleaned powders were dried in a vacuum overnight at 80 °C until complete evaporation of the solvent was achieved and the ZnS nanoparticles prepared. For the preparation of ZnS:Eu nanoparticles, the only difference during synthesis was addition of $Eu(NO_3)_3$ to the $Zn(CH_3COO)_2$ solution. The molar ratio of Eu^{3+}:Zn^{2+} was 3:100.

The as-made ZnS and ZnS:Eu nanoparticles had so faint an emission that it was almost below the detectable range of the F4500 spectrometer. The reason for this was ascribed to there being few defects in the as-made ZnS and ZnS:Eu nanoparticles. To get stronger emission, ZnS and ZnS:Eu nanoparticles were annealed for 15 min under the protection of sulfur and carbon reduction atmospheres at different temperatures. After rapid cooling down to room temperature, ZnS and ZnS:Eu nanophosphors were obtained.

Crystalline structure was characterized by the X-ray powder diffraction (XRD) technique. The PL and photoluminescence excitation (PLE) spectra were recorded using a Hitachi F-4500 fluorescence spectrometer. All measurements were conducted at room temperature.

Results and discussion

Experimental results

Figure 1 shows the XRD patterns of ZnS nanoparticle precursors and annealed ZnS nanophosphors. For the ZnS nanoparticle precursors, three diffraction peaks that corresponded to the (111), (220) and (311) plane of the zincblende phase (Powder Diffraction File, Card No. 5–566), clearly appeared, indicating the pure cubic crystal structure of ZnS nanoparticle precursors. For the annealed ZnS nanophosphors, however, the mixed phases of cubic and hexagonal, but mainly cubic, structures appeared (7), meaning that there was phase transition to a hexagonal crystal structure during annealing.

Figure 2 shows the PL and PLE spectra of ZnS and ZnS:Eu nanophosphors annealed at different temperatures. A blue emission band centered at 460 nm and a green emission band centered at 520 nm were observed that consisted of the PL spectra of ZnS (Fig. 2a) and ZnS:Eu (Fig. 2c) nanophosphors. The 460 nm emission is the well known self-activated (SA) luminescence of ZnS, and the SA center was related to Zn^{2+} vacancies (6,7). The 520 nm emission was assigned to electron transfer from sulfur vacancies to interstitial sulfur states (8). Therefore, both the 460 nm and 520 nm emissions belong to defects in ZnS luminescence.

Figure 2(b) and (d) show the PLE spectra of ZnS and ZnS:Eu nanophosphors, respectively. An excitation peak at 337 nm (3.68 eV) was observed that corresponded to the absorption of the near band-edge free excitons of ZnS, and appeared in the spectra of both the ZnS and ZnS:Eu nanophosphors. Different excitation characteristics, however, appeared in the long wavelength range of spectra of the two nanophosphors. In ZnS nanophosphors, there was no excitation signal at wavelengths $\lambda_{ex} > 337$ nm (Fig. 2b), while in ZnS:Eu nanophosphors two excitation bands appeared that were centered at 365 nm and 410 nm (Fig. 2d). The 365 nm excitation band was assigned to electron transition absorption from the Eu^{2+} acceptor level to the CB of ZnS (9) and the 410 nm excitation band to the intra-ion transition absorption $4f^7 \rightarrow 4f^6 5d^1$ of Eu^{2+} (9,10). In addition, the 365 nm and 410 nm excitation bands contributed to the 460 nm and 520 nm emissions, respectively (shown in Fig. 2e), which is consistent with the excitation characteristics of Eu^{2+} in ZnS: Eu^{2+} nanowires (9). Therefore, we show here convincing evidence that Eu^{2+} ions had been successfully doped into ZnS:Eu nanophosphors.

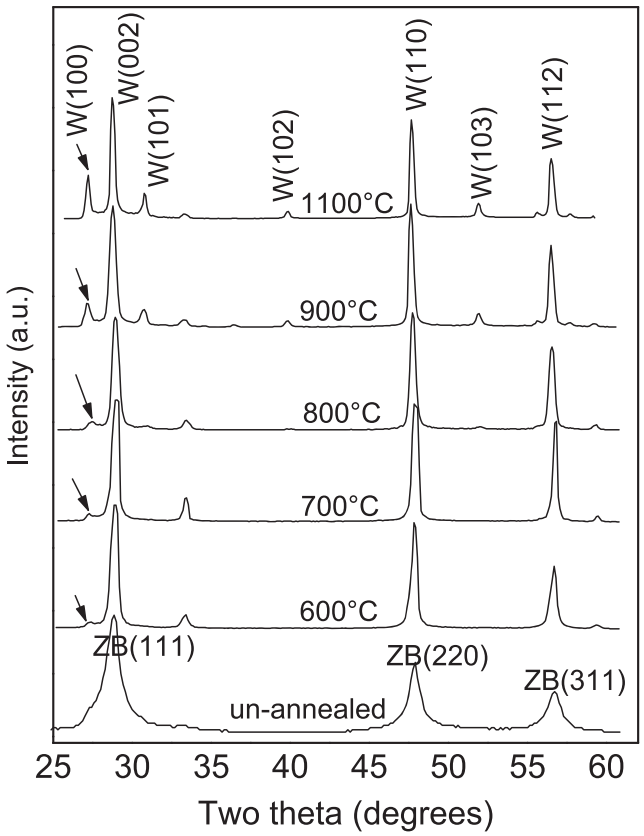

Figure 1. XRD patterns of ZnS nanoparticle precursors and ZnS nanophosphors annealed at different temperatures. The occurrence of the (100) planes of hexagonal phase (marked with an arrow) indicates the structure transition of ZnS nanophosphors at annealing temperature > 600 °C.

To further reveal the influences of Eu^{2+}-doping on 460 nm and 520 nm emissions, Fig. 3 shows the PL spectra of ZnS:Eu nanophosphors excited at different wavelengths (λ_{ex} = 410, 390, 370, 350, or 330 nm). For comparison, the PL spectrum of ZnS nanophosphors excited at 330 nm is also shown. Compared with ZnS nanophosphors, emissions in ZnS:Eu nanophosphors at 460 nm and 520 nm increased in intensity more than 10 times. Furthermore, the 520 nm emission was more prominent in the ZnS:Eu nanophosphor spectra, illustrating the relative enhancement of the 520 nm emission in ZnS:Eu nanophosphors.

Discussion

During the thermal annealing process, Eu^{3+} ions can be reduced to Eu^{2+} in ZnS:Eu nanophosphors by obtaining electrons from the surrounding S^{2-} ions. The S^{2-} ions, after losing electrons, become sulfur atoms and diffuse into the interstitial lattice (I_S), leaving a vacancy (V_S) on the site position. The reactions are as follows:

- $S^{2-} \rightarrow S + e$ $S \rightarrow I_S + V_S$
- $Eu^{3+} + e \rightarrow Eu^{2+}$

A sulfur vacancy and the IS atoms were generated in pairs and were located near to the Eu^{2+} ions (see Fig. 4a). The energy

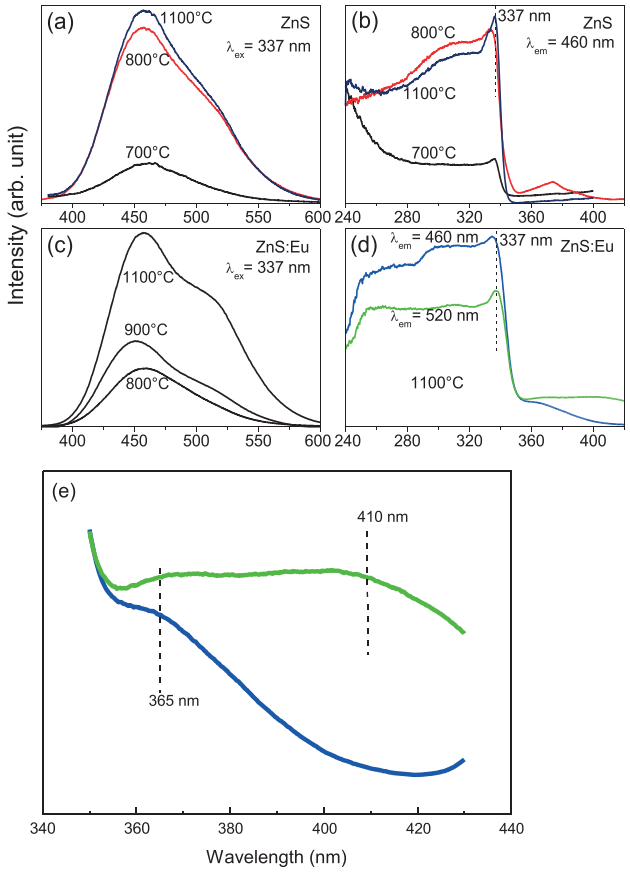

Figure 2. PL (a) and PLE (b) spectra of ZnS nanophosphers; and PL (c) and PLE (d) spectra of ZnS:Eu nanophosphors annealed at different temperatures. ZnS:Eu nanophosphors in (d) were annealed at 1100 °C; (e) is an enlargement of (d) in the wavelength range 350–430 nm.

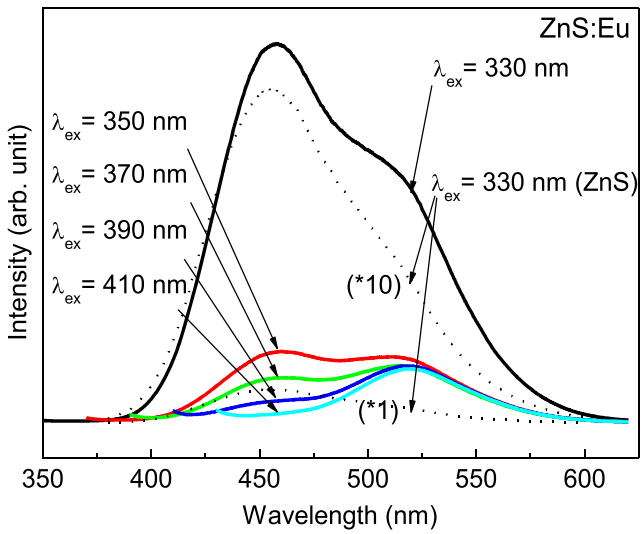

Figure 3. The PL spectra of ZnS:Eu nanophosphors excited at different wavelengths (the solid lines). The dashed lines represent the PL spectra of ZnS nanophosphors excited at 330 nm that showed 10 times intensity, and without enlargement. The ZnS and ZnS:Eu nanophosphors were annealed at 1100 °C.

absorbed by Eu^{2+} was due to intra-ion transition (corresponding to the 410 nm excitation band) and can be transferred efficiently to the surrounding sulfur vacancy because of the relatively short distance between them, leading to a relative enhancement of the

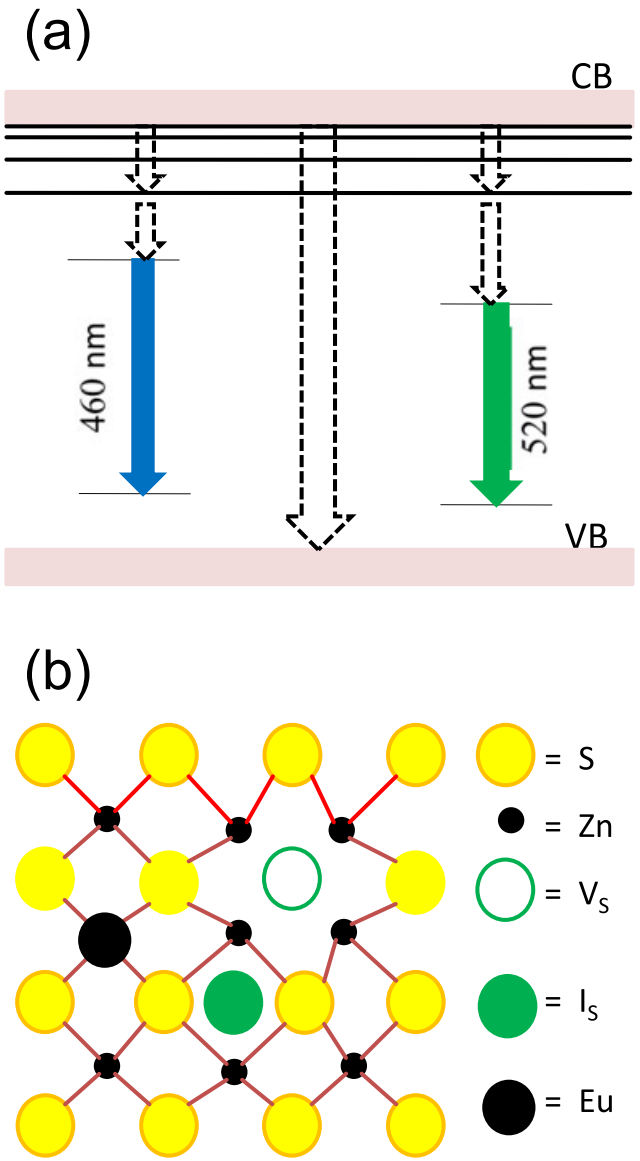

Figure 4. Electronic relaxation mechanisms for the 460 nm and 520 nm emissions. (a) Schematics of Eu^{2+} ions substituting Zn^{2+} and geminating the generation of a sulfur vacancy (V_S) and an interstitial sulfur atom (I_S) near the Eu^{2+} ions in ZnS:Eu nanophosphors. (b) Different electron relaxation processes in ZnS and ZnS:Eu nanophosphors. The dashed line arrows represent electron relaxation and the black thick lines represent the excited levels of Eu^{2+} acceptor-bound excitons. In ZnS nanophosphors, most of the electrons in the CB are relaxed and non-radiative to the VB, leading to poor 460 nm and 520 nm emissions. In the ZnS:Eu nanophosphors, most of the electrons in the CB were relaxed to the upper levels of the 460 nm and 520 nm emissions via the excited levels of Eu^{2+} acceptor-bound excitons, and leading to the strong 460 nm and 520 nm emissions.

520 nm emission. Therefore, intra-ion transition excitation of Eu^{2+} and subsequent energy transfer to the sulfur vacancy lead to a relative enhancement in the 520 nm emission in ZnS:Eu nanophosphors.

In ZnS nanophosphors, electrons in the VB are pumped into the CB at the wavelength $\lambda_{ex} < 337$ nm. However, most electrons in the CB may be relaxed and non-radiative to the VB, and only few can be relaxed to the upper levels of the 460 nm and 520 nm emissions and then give out emission. This process explains the weak luminescence in ZnS nanophosphors. Therefore, non-radiative electronic relaxation from the CB to the VB may be the cause of poor emission in ZnS nanophosphors.

LUMINESCENCE
The Journal of Biological and Chemical Luminescence

In ZnS:Eu nanophosphors, however, the 460 nm and 520 nm emissions are dramatically increased in intensity, which can be ascribed to the change in electronic relaxation processes. As demonstrated in Fig. 2(d), the 365 nm excitation band occurs that illuminates the formation of Eu^{2+} isoelectronic acceptors in ZnS:Eu nanophosphors. Furthermore, holes are readily bound with electrons near these Eu^{2+} isoelectronic acceptors and Eu^{2+} acceptor-bound excitons are therefore formed (9). As the excited levels of Eu^{2+} acceptor-bound excitons are located just below the conduction band bottom of ZnS (9), electrons in the CB are readily transferred to the excited levels of Eu^{2+} acceptor-bound excitons, via which they are further relaxed to the upper levels of the 460 nm and 520 nm emissions, leading to the 460 nm and 520 nm emissions. In above processes, the excited levels of Eu^{2+} acceptor-bound excitons serve as the intermediate state of electronic relaxation and decrease non-radiative electronic relaxation from the CB to the VB, leading thus to the strong 460 nm and 520 nm emissions. The different electronic relaxation processes in the two nanophosphors are illustrated in Fig. 4(b).

Conclusions

ZnS and ZnS:Eu nanophosphors were prepared by annealing the corresponding nanoparticle precursors synthesized by a chemical co-precipitation method. The 460 nm and 520 nm emissions were increased in intensity by more than 10 times in ZnS:Eu nanophosphors compared with ZnS nanophosphors and also, the 520 nm emission was relatively enhanced in ZnS:Eu nanophosphors. It is believed that the absorption of Eu^{2+} intra-ion transitions and subsequent energy transfer to sulfur vacancy led to the relative enhancement of the 520 nm emission in ZnS:Eu nanophosphors. Furthermore, Eu^{2+} acceptor-bound excitons are formed in ZnS:Eu nanophosphors and their excited levels serve as the intermediate state of electronic relaxation, which decreases non-radiative electronic relaxation from the CB to the VB and thus increases the intensity of the 460 nm and 520 nm emissions dramatically. In summary, the results in this work indicate a new mechanism for the enhancement of defect luminescence of ZnS in the Eu^{2+}-doped ZnS nanophosphors.

Acknowledgements

This study was financially supported by the Collaborative Innovation Center of Advanced Functional Materials (No. XTZX103732015014) and the Natural Science Research Key Project of Anhui Province University, China (No. KJ2010A303).

References

1. Yang P, Lü MK, Xü D, Yuan DL, Zhou GJ. ZnS nanocrystals co-activated by transition metals and rare-earth metals—a new class of luminescent materials. J Lumin 2001;93:101–5.
2. Sridevi D, Rajendran KV. Enhanced photoluminescence of ZnS nanoparticles doped with transition and rare earth metallic ions. Chalcogenide Lett 2010;7:397–401.
3. Ashwini K, Pandurangappa C, Nagabhushana BM. Synthesis and optical properties of undoped and Eu-doped ZnS nanoparticles. Phys Scr 2012;85:065706–10.
4. Ashwini K, Yashaswini PC. Solvothermal synthesis, characterization and photoluminescence studies of ZnS: Eu nanocrystals. Opt Mater 2014;37:537–42.
5. Ma L, Jiang K, Liu XT, Chen W. A violet emission in ZnS:Mn,Eu: luminescence and applications for radiation detection. J Appl Phys 2014;115:103104–9.
6. Vacassy R, Scholz SM, Dutta J, Plummer CJG, Houriet R, Hofmann H. Synthesis of controlled spherical zinc sulfide particles by precipitation from homogeneous solutions. J Am Ceram Soc 1998;81:2699–705.
7. Dinsmore AD, Hsu DS, Qadri SB, Cross JO, Kennedy TA, Gray HF, Ratna BR. Structure and luminescence of annealed nanoparticles of ZnS:Mn. J Appl Phys 2000;88:4985–93.
8. Wang X, Shi J, Feng Z, Li M, Li C. Visible emission characteristics from different defects of ZnS nanocrystals. Phys Chem Chem Phys 2011;13:4715–23.
9. Cheng BC, Wang ZG. Synthesis and optical properties of europium-doped ZnS: long-lasting phosphorescence from aligned nanowires. Adv Funct Mater 2005;15:1883–90.
10. Chen W, Malm JO, Zwiller V, Huang Y, Liu S, Wallenberg R, Bovin JO, Samuelson L. Energy structure and fluorescence of Eu^{2+} in ZnS:Eu nanoparticles. Phys Rev B 2000;61:11021–4.

